

## Vertical structure of warming consistent with an upward shift in the middle and upper troposphere

Paul A. O’Gorman<sup>1</sup> and Martin S. Singh<sup>1</sup>

Received 21 February 2013; accepted 6 March 2013; published 9 May 2013.

[1] Warming in climate-change simulations reaches a local maximum in the tropical upper troposphere as expected from moist-adiabatic lapse rates. But the structure of warming varies between models and differs substantially from moist adiabatic in the extratropics. Here, we relate the vertical profile of warming to the climatological temperature profile using the vertical-shift transformation (VST). The VST captures much of the intermodel scatter in the ratio of upper- to middle-tropospheric warming in both the extratropics and tropics of simulations from the Coupled Model Intercomparison Project 5 (CMIP5). Application of the VST to observed climatological temperatures yields warming ratios that are in the range of what is obtained from the model climatological temperatures, although biases in some model climatologies lead to substantial errors when shifted upward. Radiosonde temperature trends are consistent with an upward shift in recent decades in the Northern Hemisphere, with less-robust results in the Southern Hemisphere. **Citation:** O’Gorman, P. A., and M. S. Singh (2013), Vertical structure of warming consistent with an upward shift in the middle and upper troposphere, *Geophys. Res. Lett.*, 40, 1838–1842, doi:10.1002/grl.50328.

### 1. Introduction

[2] The vertical structure of atmospheric warming under climate change is important because of its radiative effects and because it affects convection and large-scale circulations through the static stability. Considerable attention has been devoted to discrepancies between the vertical structure of tropical warming in observations and climate-model simulations [Thorne *et al.*, 2011]. At least some of these discrepancies are thought to relate to the difficulty of reliably calculating observed trends [Santer *et al.*, 2005]. Modern climate models robustly simulate amplified upper-tropospheric warming in the tropics, but intermodel differences persist in the degree of amplification [Fu *et al.*, 2011]. Different responses may result from variability, differences in forcings, and intrinsic model differences such as in the parameterization of moist convection [Schlesinger and Mitchell, 1987]. In particular, assumptions regarding cloud radiative effects and convective entrainment affect the relationship between temperatures in the upper and lower tropical troposphere [Ramaswamy and Ramanathan,

1989; Held *et al.*, 2007], and the degree of amplified upper-tropospheric warming is correlated with model biases in upper-tropospheric temperatures [Po-Chedley and Fu, 2012].

[3] Moist-adiabatic lapse rates provide a useful theoretical standard with which to compare temperature changes in the tropics [e.g., Santer *et al.*, 2005], but it is not clear that they can help explain intermodel differences in the vertical structure of warming, and they are not applicable to mean lapse rates in the extratropics because of the effects of baroclinic eddies [e.g., Schneider and O’Gorman, 2008]. Theories of the moist extratropical stratification relate broad measures of the static stability to meridional temperature gradients [e.g., Juckes, 2000; Schneider and O’Gorman, 2008; Frierson, 2008; O’Gorman, 2011], but they can only provide limited information about the detailed structure of warming.

[4] A promising alternative is to consider the response of tropospheric temperatures to global warming as involving an upward shift. Upward shifts of the dry static stability with warming were found in simulations with general circulation models (GCMs) in the southern midlatitudes [Kushner *et al.*, 2001] and near the tropopause [Lorenz and DeWeaver, 2007]. However, Singh and O’Gorman [2012] showed that a pure upward shift of temperature is thermodynamically inconsistent because latent heating does not shift upward consistently. They instead introduced the vertical-shift transformation (VST) which describes a coherent upward shift with warming of winds, relative humidity, and saturation specific humidity. According to the VST, the transformation of temperature involves both an upward shift and an additional term that is necessary given the pure upward shift of saturation specific humidity. In simulations of warming climates with an idealized GCM and in a multimodel mean from CMIP3, the VST was found to capture many of the simulated changes above 600 hPa, especially for temperatures and relative humidities [Singh and O’Gorman, 2012].

[5] Here we apply the VST to simulations from CMIP5 and show that it also captures intermodel scatter in the vertical structure of warming. We apply the VST to observed climatological temperatures to determine the importance of model climatological biases, and we examine the extent to which observed temperature trends in recent decades conform to an upward shift according to the VST. We consider the vertical structure of warming at all latitudes since the VST is not specific to the dynamics of the tropics or extratropics.

### 2. Vertical-Shift Transformation (VST)

[6] Given a solution of the moist primitive equations and a rescaling parameter  $\beta > 1$ , the VST gives a new

Additional supporting information may be found in the online version of this article.

<sup>1</sup>Department of Earth, Atmospheric, and Planetary Sciences, Massachusetts Institute of Technology, Cambridge, Massachusetts, USA.

Corresponding author: P. A. O’Gorman, Massachusetts Institute of Technology, Cambridge, MA 02139, USA. (pog@mit.edu)

approximate solution that is shifted upward from pressure  $\beta p$  to  $p$ . For a small vertical shift ( $\beta$  close to one), the VST may be linearized to give an expression for the temperature change  $\delta T$  that is proportional to  $\beta - 1$ ,

$$\delta T_{\text{VST}} = (\beta - 1) \left( p \frac{\partial T}{\partial p} - \frac{R_v T^2}{L} \right), \quad (1)$$

where  $R_v$  is the gas constant for water vapor and  $L$  is the latent heat of vaporization or sublimation of water (cf. section 2f of *Singh and O’Gorman* [2012]). The term proportional to the pressure derivative of temperature in (1) relates to the vertical shift, and the term proportional to  $T^2$  relates to the effects of water vapor.

[7] The transformation parameter  $\beta$  is constant in the vertical, which implies that the vertical structure of warming given by (1) is independent of the magnitude of the vertical shift. In particular, ratios of temperature changes at different pressure levels [e.g.,  $\delta T_{\text{VST}}(300 \text{ hPa})/\delta T_{\text{VST}}(500 \text{ hPa})$ ] depend only on the climatological temperature profile with no tunable parameters.

[8] Limitations of the VST include the assumption in its derivation that the radiative cooling rate shifts upward with the specific humidity, and the inability of the transformation to satisfy the surface boundary conditions on winds and humidity [*Singh and O’Gorman*, 2012]. As a result, we focus on the middle and upper troposphere where the upward shift of the radiative cooling with humidity is most likely to be valid and the effects of the lower boundary are relatively weak. In applying (1), we evaluate the pressure derivative by first interpolating the vertical temperature profile using a cubic spline, and we interpolate  $L$  in a mixed-phase range between values appropriate for ice and liquid [*Simmons et al.*, 1999].

### 3. Climate Models

[9] We examine the extent to which the VST captures intermodel scatter in the vertical warming profiles in historical simulations with 25 coupled climate models drawn from CMIP5. The VST (expression 1) is applied to climatological temperatures averaged from 1960 to 2005 and compared to temperature trends over the same period. The slightly shorter period 1960–2004 is used for two models as specified in Table S1 in the supporting information. Linear least-squares trends are calculated based on monthly anomalies at each latitude, longitude, and level prior to averaging. Anomalies are calculated relative to the seasonally varying climatology as estimated over the same period.

[10] We first consider tropical temperature trends averaged zonally and in latitude between  $20^\circ\text{S}$  and  $20^\circ\text{N}$  with area weighting (Figure 1). The VST captures the profile of warming over the middle and upper troposphere, including the increase in warming with height from the lower troposphere to a local maximum near 250 hPa, and the transition to a cooling near 100 hPa (Figure 1a). This agreement between the VST and simulations is consistent with the results of *Singh and O’Gorman* [2012] for the earlier CMIP3 simulations. Here we see that the VST also captures intermodel differences in the vertical structure of warming, as shown for two models with very different warming profiles in Figure 1a. The amplification of warming in the upper troposphere is much more pronounced in MIROC5 (blue line) compared with INMCM4 (black line), and this

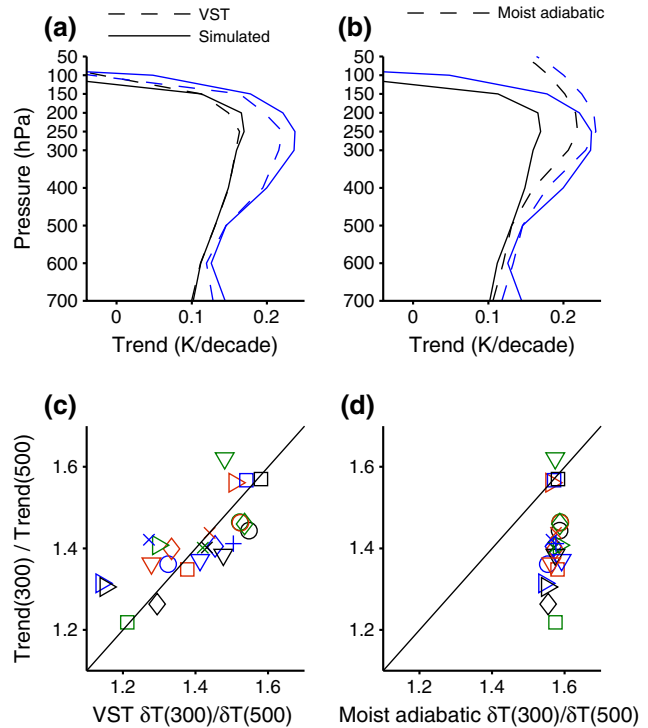


**Figure 1.** (a, b) Tropical ( $20^\circ\text{S}$  to  $20^\circ\text{N}$ ) temperature trends versus pressure in simulations with two climate models (solid lines) and the corresponding temperature changes according to the VST (dashed lines in Figure 1a) and a moist-adiabatic lapse rate (dashed lines in Figure 1b). For the purposes of presentation, the VST and moist-adiabatic profiles are rescaled to match the temperature trends at 500 hPa. (c, d) Ratio of temperature trends at 300 hPa and 500 hPa in the simulations versus the same ratio according to the VST (in Figure 1c) and a moist-adiabatic lapse rate (in Figure 1d). The models shown in Figures 1a and 1b are the models with the lowest (INMCM4, black lines) and highest (MIROC5, blue lines) ratios of temperature trends at 300 hPa and 500 hPa. The models shown in Figures 1c and 1d are identified in Table S1.

difference is captured by the VST. To quantify the applicability of the VST across models, Figure 1c shows the ratio of temperature trends at 300 hPa to 500 hPa in all of the model simulations. The VST gives a good estimate of this ratio across the models and captures much of the intermodel scatter (the correlation coefficient across models is 0.75). Using a pure upward shift of temperature rather than the VST yields less accurate warming ratios that are lower by roughly 0.2.

[11] The assumption of a moist-adiabatic lapse rate is consistent with the amplified warming in the upper troposphere in the simulations (Figure 1b), but it does not capture the temperature changes above 150 hPa or the intermodel scatter (Figure 1d). The moist-adiabatic warming profiles are calculated by integrating a saturated moist adiabat to both higher and lower pressure levels starting from 500 hPa at the climatological temperature, and then repeating the integrations but adding to the initial temperature the temperature trend at 500 hPa times the duration of the time period. A pseudoadiabat is assumed, ice is treated using a mixed phase [*Simmons et al.*, 1999], and we compare temperatures

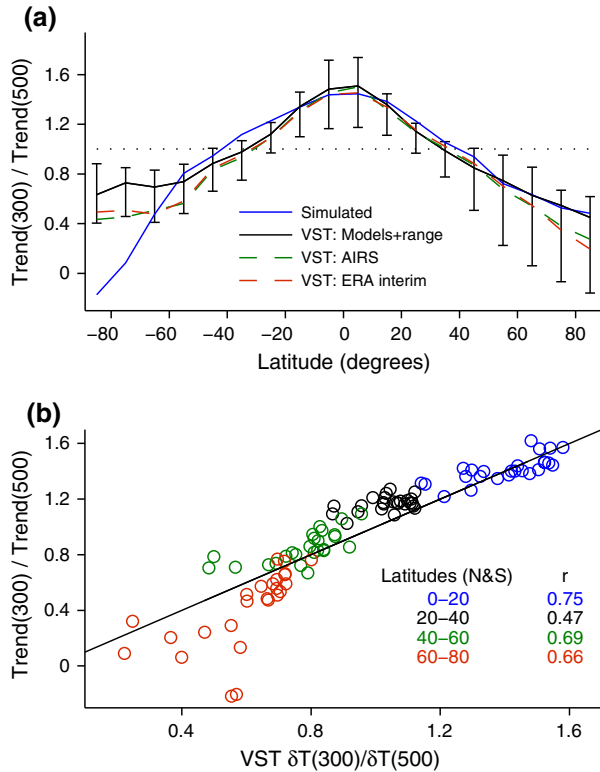


**Figure 2.** (a) Ratio of temperature trends at 300 hPa and 500 hPa versus latitude in the CMIP5 simulations (blue line shows the multimodel median of ratios) and for the VST applied to the model climatologies (black line shows the multimodel median of ratios; bars show the model range), the AIRS climatology (green dashed line), and the ERA-Interim climatology (red dashed line). (b) Warming ratios (300 hPa and 500 hPa) for individual climate models; the ratio of simulated trends is plotted versus the ratio of temperature changes implied by the VST and the model climatologies. Results in Figure 2b have been averaged over different latitude bands and between the Northern and Southern Hemispheres to reduce noise. The solid line corresponds to equal transformed and simulated ratios. The correlation coefficient ( $r$ ) across models for each latitude band is given in the legend.

rather than virtual temperatures. Different moist-adiabatic warming profiles are obtained if different assumptions are made regarding reversibility, the mixed phase, and whether temperatures or density temperatures are used, but no one moist adiabat is found to capture the intermodel scatter. Nonetheless, some of the intermodel scatter could result from different moist adiabats being appropriate in different climate models.

[12] The ratio of warming at 300 hPa and 500 hPa is consistent with what is given by the VST at all latitudes except near Antarctica (Figure 2a), with more warming at 300 hPa than 500 hPa in the tropics and subtropics, and more warming at 500 hPa than 300 hPa at higher latitudes. That the VST captures the warming profiles in the extratropics is noteworthy since, for example, moist-adiabatic lapse rates are not expected to be a useful guide for the extratropical stratification [e.g., Schneider and O’Gorman, 2008]. The levels 300 hPa and 500 hPa were chosen as they remain just inside

the troposphere at all latitudes while still being in the part of the troposphere where the VST seems to be most applicable. Intermodel scatter is also well captured except at very high latitudes (Figure 2b). Correlation coefficients for each latitude band are given in the legend of Figure 2b and range from 0.47 to 0.75. Note that this good agreement across models and latitudes is obtained using the VST with no free parameters.

[13] Similar results are obtained for the forcing scenario RCP8.5 (Figures S1 and S2) but with generally better agreement between the warming profiles and the VST than for the more weakly forced historical simulations. The correlation coefficients range from 0.59 to 0.91 for different latitude bands (compared to 0.47 to 0.75 for the historical trends), and the ratios from the different latitude bands and models almost all collapse onto the one-to-one line (Figure S2). As discussed in the supplementary text, the full rather than linearized VST is needed for RCP8.5 because of the size of the temperature changes.

[14] The discrepancies between the VST and the simulated historical trends near Antarctica (Figure 2a) do not occur under RCP8.5 (Figure S2). These discrepancies are less pronounced in historical simulations with only greenhouse-gas forcing and no changes in ozone (Figure S3), and they may also relate to the simulated fast response to increasing  $\text{CO}_2$  concentrations which involves a cooling at 300 hPa at high southern latitudes [Colman and McAvaney, 2011].

[15] Agreement between the warming ratios from the simulations and the VST drops off for levels closer to the surface or near the stratosphere (Figure S4). Extension of the VST to be applicable to the lower troposphere is desirable but entails the difficult theoretical problem of including the effects of the boundary layer and the lower boundary conditions.

#### 4. Application of VST to Observed Climatology

[16] To the extent that climatological temperatures in the model simulations are biased, the VST will predict different warming profiles based on climatological temperatures from observations and models. It is interesting, therefore, to apply the VST to observed climatological temperatures, especially as time-mean temperatures are more reliably observed and less subject to natural variability compared with temperature trends over the past few decades.

[17] We consider temperatures from the Atmospheric Infrared Sounder (AIRS) over the period 2003–2011 [Fetzer, 2006], using the V5 L3 standard monthly product which also includes inputs from the Advanced Microwave Sounding Unit. The temperatures are first averaged in time and then zonally, but values within 100 hPa of the surface in the time mean are excluded from the zonal mean. Ascending and descending passes are included when available. We also consider zonal- and time-mean temperatures from the ERA-interim reanalysis over the period 1979–2011 [Dee et al., 2011]. Application of the VST yields similar ratios of warming at 300 hPa and 500 hPa regardless of whether the AIRS or ERA-interim climatological temperatures are used (Figure 2a).

[18] We then compare the ratios based on the VST applied to observed climatological temperatures with the ratios based on the VST applied to climatological

temperatures from the historical simulations (Figure 2a). The ratios based on observational climatologies generally fall within the intermodel scatter of the ratios based on model climatologies (shown by black bars in Figure 2a). However, the model scatter is quite large at some latitudes, so that biases in the climatological temperature profiles in some of the models will lead to substantial errors when shifted upward according to the VST.

## 5. Radiosonde Trends

[19] We examine whether observed temperature trends over the period 1960–2005 are consistent with an upward shift according to the VST. We focus primarily on the RICH- $\tau$  radiosonde dataset (V1.5.1) which has been homogenized using reanalysis background forecasts and comparison with neighboring stations [Haimberger *et al.*, 2008, 2012]. The radiosonde observations are sparse in the tropics and Southern Hemisphere, but, to the extent that the VST is applicable at all latitudes and longitudes, a consistent comparison may be made by calculating both the trends and VST-implied trends using only the same observations.

[20] Our results are based on medians across station time series (including both daily observation times) in 15° latitude bands starting with a band centered on 75°S. Results at latitudes with very sparse data may be sensitive to the choice of latitude bands, especially if the latitude bands are too narrow. Time series are excluded if less than 180 monthly values are available. For each latitude band, the median of the ratio of trends at 300 hPa and 500 hPa is calculated, with trends calculated as in section 3. Reporting medians rather than means of the ratios helps to minimize the influence of remaining artifacts [cf. Sherwood *et al.*, 2008].

[21] The temperature changes implied by the VST are calculated based on time-mean temperatures at each station and observation time, and the median for each latitude band of the ratio of temperature changes at 300 hPa and 500 hPa is then calculated. For consistency, only stations contributing to the trend ratios are included when applying the VST.

[22] The warming ratios for the trends and the VST show reasonably good agreement in the Northern Hemisphere, with worse agreement in the Southern Hemisphere as might be expected given the much smaller number of stations there (Figure 3). Similar results are found if the end year of the analysis is extended from 2005 to 2011 (Figure S5). We also calculate trend ratios for the same station time series but without the homogenization adjustments. The agreement with the VST for these “raw” time series is as good (or even slightly improved in the Southern Hemisphere) when compared with the homogenized time series (Figure 3). Comparison with other variants of the homogenization method [Haimberger *et al.*, 2012] and the iterative universal kriging (IUK) dataset of Sherwood *et al.* [2008] shows that the trend ratios are more robust in the Northern Hemisphere than in the Southern Hemisphere, particularly at high latitudes (Figure S6).

[23] Overall, the radiosonde trends are supportive of an upward shift of middle- and upper-tropospheric temperatures in recent decades, at least in the Northern Hemisphere. We caution that substantially worse agreement is found if means rather than medians are considered or if trends are calculated over much shorter time periods.

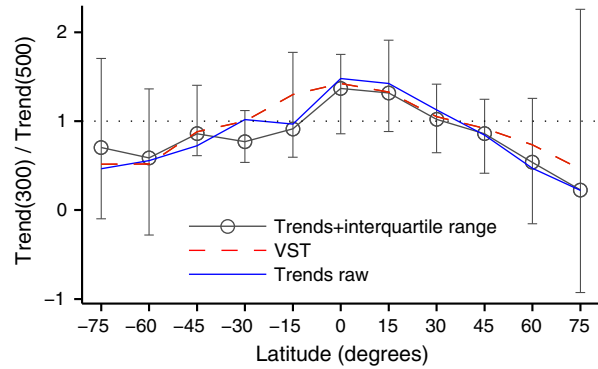


**Figure 3.** Ratio of temperature trends at 300 hPa and 500 hPa versus latitude based on the RICH- $\tau$  radiosonde dataset. The gray line with circles shows ratios based on trends over the period 1960–2005. The dashed red line shows the ratios based on the VST and the RICH- $\tau$  climatology over the same period. Results are shown for medians of the ratios over all station time series in 15° latitude bands. Vertical bars indicate interquartile ranges in the trend ratios. The blue line shows ratios based on trends from the raw (nonhomogenized) radiosonde time series for comparison.

## 6. Conclusions

[24] We have used the VST introduced by Singh and O’Gorman [2012] to relate the vertical structure of warming to the climatological temperature distribution in both simulations and observations. The results illustrate the value in having a theory to compare with at all latitudes. With some exceptions in the Southern Hemisphere, there is a similar meridional pattern in models, observations, and the VST as regards the vertical structure of warming in the middle and upper troposphere.

[25] The VST captures much of the intermodel scatter in the ratio of warming at 300 hPa and 500 hPa in the tropics (which a simple assumption of moist-adiabatic lapse rates does not) and in the extratropics (where moist-adiabatic lapse rates are not directly applicable). An important implication is that much of this intermodel scatter derives from factors that affect the model climatologies, such as different model parameterizations, and not just from variability or differences in radiative forcings. The role of different parameterizations in setting the vertical structure of temperature could be explored using perturbed physics experiments in future work. The link given by the VST between the climatological temperature profile and the vertical structure of warming should be helpful in understanding the effects of different choices of parameterization.

[26] Application of the VST to observed climatological temperatures results in warming ratios that fall within the range of what is obtained from the model climatologies. However, the biases in climatological temperatures in some of the models are sufficient to lead to substantial biases in response to an upward shift according to the VST.

[27] Trends based on the radiosonde datasets we have considered are broadly consistent with an upward shift according to the VST in the middle and upper troposphere in recent decades. Our results are most supportive of an upward shift in the Northern Hemisphere, since both the agreement with the VST and the robustness of the trend ratios

seem to be best in this hemisphere. Further work is needed to compare the VST with trends from other observational datasets.

[28] **Acknowledgments.** We are grateful to Darryn Waugh, Susan Solomon, Kerry Emanuel, Steven Sherwood, Dennis Hartmann, and an anonymous reviewer for helpful comments and to Leopold Haimberger for providing us with the RAOCORE/RICH V1.5.1 station time series. We acknowledge the World Climate Research Programme's Working Group on Coupled Modelling, which is responsible for CMIP, and we thank the climate modeling groups for producing and making available their model output. For CMIP, the U.S. Department of Energy's Program for Climate Model Diagnosis and Intercomparison provides coordinating support and led development of software infrastructure in partnership with the Global Organization for Earth System Science Portals. The AIRS data used in this study are archived and distributed by the Goddard Earth Sciences Data and Information Services Center and were acquired as part of the activities of NASA's Science Mission Directorate. European Centre for Medium-Range Weather Forecasts (ECMWF) ERA-Interim data were obtained from the ECMWF data server. We are grateful for support from NSF grant AGS-1148594.

## References

- Colman, R. A., and B. J. McAvaney (2011), On tropospheric adjustment to forcing and climate feedbacks, *Clim. Dyn.*, *36*, 1649–1658.
- Dee, D. P., et al. (2011), The ERA-Interim reanalysis: Configuration and performance of the data assimilation system, *Q. J. R. Meteorol. Soc.*, *137*, 553–597.
- Fetzer, E. J. (2006), Preface to special section: Validation of Atmospheric Infrared Sounder observations, *J. Geophys. Res.*, *111*, D09S01, doi:10.1029/2005JD007020.
- Frierson, D. M. W. (2008), Midlatitude static stability in simple and comprehensive general circulation models, *J. Atmos. Sci.*, *65*, 1049–1062.
- Fu, Q., S. Manabe, and C. M. Johanson (2011), On the warming in the tropical upper troposphere: Models versus observations, *Geophys. Res. Lett.*, *38*, L15704, doi:10.1029/2011GL048101.
- Haimberger, L., C. Tavalato, and S. Sperka (2008), Toward elimination of the warm bias in historic radiosonde temperature records—Some new results from a comprehensive intercomparison of upper-air data, *J. Climate*, *21*, 4587–4606.
- Haimberger, L., C. Tavalato, and S. Sperka (2012), Homogenization of the global radiosonde temperature dataset through combined comparison with reanalysis background series and neighboring stations, *J. Climate*, *25*, 8108–8131.
- Held, I. M., M. Zhao, and B. Wyman (2007), Dynamic radiative-convective equilibria using GCM column physics, *J. Atmos. Sci.*, *64*, 228–238.
- Jukes, M. N. (2000), The static stability of the midlatitude troposphere: The relevance of moisture, *J. Atmos. Sci.*, *57*, 3050–3057.
- Kushner, P. J., I. M. Held, and T. L. Delworth (2001), Southern Hemisphere atmospheric circulation response to global warming, *J. Climate*, *14*, 2238–2249.
- Lorenz, D. J., and E. T. DeWeaver (2007), Tropopause height and zonal wind response to global warming in the IPCC scenario integrations, *J. Geophys. Res.*, *112*, D10119, doi:10.1029/2006JD008087.
- O'Gorman, P. A. (2011), The effective static stability experienced by eddies in a moist atmosphere, *J. Atmos. Sci.*, *68*, 75–90.
- Po-Chedley, S., and Q. Fu (2012), Discrepancies in tropical upper tropospheric warming between atmospheric circulation models and satellites, *Environ. Res. Lett.*, *7*, 044018.
- Ramaswamy, V., and V. Ramanathan (1989), Solar absorption by cirrus clouds and the maintenance of the tropical upper troposphere thermal structure, *J. Atmos. Sci.*, *46*, 2293–2310.
- Santer, B. D., et al. (2005), Amplification of surface temperature trends and variability in the tropical atmosphere, *Science*, *309*, 1551–1556.
- Schlesinger, M. E., and J. F. B. Mitchell (1987), Climate model simulations of the equilibrium climatic response to increased carbon dioxide, *Rev. Geophys.*, *25*, 760–798.
- Schneider, T., and P. A. O'Gorman (2008), Moist convection and the thermal stratification of the extratropical troposphere, *J. Atmos. Sci.*, *65*, 3571–3583.
- Sherwood, S. C., C. L. Meyer, R. J. Allen, and H. A. Titchner (2008), Robust tropospheric warming revealed by iteratively homogenized radiosonde data, *J. Climate*, *21*, 5336–5350.
- Simmons, A. J., A. Untch, C. Jakob, P. Källberg, and P. Undén (1999), Stratospheric water vapour and tropical tropopause temperatures in ECMWF analyses and multi-year simulations, *Quart. J. Roy. Meteor. Soc.*, *125*, 353–386.
- Singh, M. S., and P. A. O'Gorman (2012), Upward shift of the atmospheric general circulation under global warming: Theory and simulations, *J. Climate*, *25*, 8259–8276.
- Thorne, P. W., J. R. Lanzante, T. C. Peterson, D. J. Seidel, and K. P. Shine (2011), Tropospheric temperature trends: History of an ongoing controversy, *WIREs Clim. Change*, *2*, 66–88.